

He II REIONIZATION AND SOURCES OF METAGALACTIC IONIZATION

J. Michael Shull

CASA, Department of Astrophysical and Planetary Sciences, University of Colorado, Boulder, CO 80309 (mshull@casa.colorado.edu)

Abstract. Intergalactic Ly α opacity suggests that H I was reionized at $z \approx 6$, while He II reionization was delayed to $z \approx 3$. Both epochs are in conflict with inferences from CMB optical depth (WMAP) which suggest early reionization at $z = 10 - 20$. One of the major contributions of *FUSE* to cosmological studies has been the detection of He II Ly α (“Gunn-Peterson”) absorption in the spectra of AGN at redshifts $z \geq 2.03$. Spectra of He II absorbers, taken in concert with corresponding H I (Ly α) lines, allow us to fix the epoch of helium reionization at $z_{\text{HeII}} \approx 2.8 \pm 0.2$. Here, I review *FUSE* observations of He II absorption, together with their implications for the sources and transport of ionizing radiation over 30-50 Mpc distances through the IGM. *FUSE* observations of He II absorption toward HE 2347-4342, combined with *Keck* and *VLT* observations of H I, are consistent with photoionization by QSOs, with a wide range of intrinsic spectral indices, and modified by filtering and reprocessing in the IGM. The He II/H I ratio (η) exhibits variations over 1 Mpc distance scales ($\Delta z \approx 10^{-3}$). Intriguingly, this η -ratio is also correlated with Ly α filaments and voids. The ionizing radiation field appears to be softer (higher He II/H I) in the voids. These void regions may be ionized by local soft sources (dwarf starburst galaxies), or the QSO radiation may be softened by escape from AGN cores and transport through denser regions in the “cosmic web”. The differences in ionizing spectra may explain the 1.4 Gyr lag between H I and He II epochs.

1. Overview: Reionization of the Intergalactic Medium

Before beginning a discussion of the *FUSE* contributions to the study of He II reionization, I provide an overview of the cosmological significance of “reionization”. This term refers to the sudden increase in ionization fraction of hydrogen gas in the intergalactic medium (IGM), initiated at redshifts $z \geq 6$ by the first sources of ionizing radiation. After the epoch of recombination at $z_{\text{rec}} \approx 1300$, the IGM entered a long period of “dark ages” when the IGM was mostly neutral. This period ended sometime before $z \approx 6$, perhaps as early as $z = 10 - 20$.

The ionization state of the IGM affects the transmission of radiation through the Ly α absorbers (H I and He II), as well as the electron-scattering optical depth to the cosmic microwave background (CMB) radiation. As individual ionizing sources (stars, galaxies, quasars) began emitting ionizing radiation, regions of ionized gas were produced, preceded by ionization fronts (I-fronts) in the IGM. These isolated ionized zones (H II regions, He III regions) eventually overlapped (Gnedin 2000), after which the IGM became transparent to Ly α radiation. Residual absorption continued as a “picket fence” of discrete, redshifted Ly α absorbers, often termed the “Ly α forest” – see spectra in Songaila (1998).

The rapid increase in IGM ionization occurred as a topological phase change in the volume filling factor of ionized zones. The longer the first ionizing sources were on, the greater the volume of the zones. In order to effectively absorb all the Ly α radiation at $z = 6$ requires a neutral fraction of just $x_{\text{HI}} = 2 \times 10^{-4}$, even in gas that is underdense by a factor of 10 relative to the mean. Simulations of this reionization process (Gnedin 2000, 2004) show that the transition from neutral to ionized is quite extended in time, between $z = 5 - 10$. The first stage (pre-overlap) involves the development and expansion of the first isolated ionizing sources. The second stage marks the overlap of the I-fronts and the disappearance of the last vestiges of low-density neutral gas. Finally, in the post-overlap stage, the remaining high-density gas is photoionized from the outside. The final drop in neutral fraction and increase in photon mean free path occur quite rapidly, over $\Delta z \approx 0.3$ (see Fig. 1 of Gnedin 2004).

Reionization is tied closely to the onset of galaxy formation beginning at $z \geq 20$. For the ionization of He II, and somewhat for H I, reionization depends on the rise in the numbers and luminosities of active galactic nuclei from $z = 5 \rightarrow 2$. According to numerical simulations (e.g., Ricotti, Gnedin, & Shull 2002, hereafter denoted RGS), the earliest epochs of galaxy formation began at $z \approx 20 - 30$ triggered by H I and H₂ cooling of protogalactic halos with virial temperatures $T_{\text{vir}} = 10^3$ K to 10^4 K. RGS found that the average star formation rate density, ρ_{SFR} , increased monotonically from 10^{-3} to $10^{-1} M_{\odot} \text{ yr}^{-1} \text{ Mpc}^{-3}$ between $z = 20$ and 10, according to the approximate formula:

$$\text{SFR} = (0.003 M_{\odot} \text{ yr}^{-1} \text{ Mpc}^{-3}) 10^{(20-z)/5} . \quad (1)$$

The effects of reionization can be seen indirectly in the electron-scattering optical depth of the cosmic microwave background (CMB), as we discuss in the next section. However, the most direct observations of the IGM ionization state come from their influence on the Ly α line-blanketing opacity of the IGM at wavelengths shortward of the H I and He II Ly α lines at $(1215.670 \text{ \AA})(1+z)$ and $(303.782 \text{ \AA})(1+z)$, respectively. As the amounts of H I or He II increase, these line-blanketed regions grow into black (“Gunn-Peterson”) absorption troughs, whose presence can be used to identify high-redshift galaxies (Steidel et al. 2002). The best probes of the epoch of reionization have come from analyzing the weak transmission of AGN continuum flux in these troughs, as the high-redshift IGM transforms from a neutral to ionized medium. The He II absorption becomes detectable in the far ultraviolet at redshifts $z \geq 2.03$ with *FUSE* and at $z \geq 2.79$ with HST. From the latest Ly α data, the reionization epochs occur at $z \approx 6.1 \pm 0.3$ for H I (Becker et al. 2001; Fan et al. 2002; Gnedin 2004) and at $z \approx 2.8 \pm 0.2$ for He II (Kriss et al. 2001; Smette et al. 2002; Shull et al. 2004; Zheng et al. 2004).

2. Electron-Scattering Optical Depth of the IGM

An indirect measure of reionization can be extracted from an analysis of fluctuations in the CMB radiation, particularly the large-angle temperature-polarization correlations. By combining the first-year data from the *Wilkinson Microwave Anisotropy Probe* (WMAP) with other results on the CMB, Ly α forest, and galaxy large-scale structure, Spergel et al. (2003) found a high value of the

CMB optical depth to electron scattering, $\tau_e = 0.17 \pm 0.04$. This optical depth implies a surprisingly large redshift of early IGM reionization, ranging from $11 < z_r < 30$ at 95% confidence (Kogut et al. 2003). More recent estimates of τ_e and other cosmological parameters (Tegmark et al. 2004) combined the WMAP data with the three-dimensional power spectrum from over 200,000 galaxies in the Sloan Digital Sky Survey (SDSS). Their analysis tightened many of the WMAP error bars and gave somewhat lower $\tau_e = 0.12^{+0.08}_{-0.06}$. There is still disagreement between the redshift $z_r \approx 6$ found from (H I) Ly α opacity and the “early reionization” estimates, $z_r = 10$ -20, inferred from the CMB. The optical-depth estimates from WMAP are consistent with a wide range in τ_e , reflecting the broad likelihood function (see Figure 4 of Spergel et al. 2003). The analysis of second-year WMAP data may yield a more precise determination of τ_e .

To elucidate the dependence of τ_e on the epoch of reionization, we now provide the following simplified derivation. Assuming instantaneous, complete ionization at redshift z_r , we can write τ_e as the integral of $n_e \sigma_T dl$, the electron density times the Thomson cross section along proper length. For a standard Λ CDM cosmology, we have $(dl/dz) = c(dt/dz) = (1+z)^{-1}[c/H(z)]$, where $H(z) = H_0[\Omega_m(1+z)^3 + \Omega_\Lambda]^{1/2}$ and $\Omega_m + \Omega_\Lambda = 1$. We adopt $n_e = n_H(1+y)$ and $n_H = [(1-Y)\rho_{\text{cr}}/m_H](1+z)^3$, where $Y = 0.244$ (He mass fraction) and $y \approx 0.0807$ (He fraction by number). We further assume that helium is singly ionized (He II at $z \geq 3$). The above integral can be done exactly:

$$\begin{aligned} \tau_e &= \left(\frac{c}{H_0}\right) \left(\frac{2\Omega_b}{3\Omega_m}\right) \left[\frac{\rho_{\text{cr}}(1-Y)(1+y)\sigma_T}{m_H}\right] \left[\{\Omega_m(1+z_r)^3 + \Omega_\Lambda\}^{1/2} - 1\right] \\ &\approx (0.0376h) \left(\frac{\Omega_b}{\Omega_m}\right) \left[\{\Omega_m(1+z_r)^3 + \Omega_\Lambda\}^{1/2} - 1\right]. \end{aligned} \quad (2)$$

In the above numerical expression, we can substitute the WMAP-concordance values (Spergel et al. 2003; Bennett et al. 2003), $\Omega_b h^2 = 0.0224 \pm 0.0009$, $\Omega_m h^2 = 0.135^{+0.008}_{-0.009}$, and $h = 0.71^{+0.04}_{-0.03}$, where $h = [H_0/(100 \text{ km s}^{-1} \text{ Mpc}^{-1})]$ is the scaled Hubble constant. The critical density is $\rho_{\text{cr}} = (1.879 \times 10^{-29} \text{ g cm}^{-3})h^2$. For large redshifts, $\Omega_m(1+z)^3 \gg \Omega_\Lambda$, and the integral simplifies to

$$\tau_e \approx \left(\frac{c}{H_0}\right) \left(\frac{2\Omega_b}{3\Omega_m}\right) \left[\frac{\rho_{\text{cr}}(1-Y)(1+y)\sigma_T}{m_H}\right] \Omega_m^{1/2} (1+z_r)^{3/2} \approx (0.00229)(1+z_r)^{3/2}, \quad (3)$$

nearly independent of h . Additional contributions to τ_e arise from residual electrons ($10^{-3.3}$ ionized fraction) frozen out after recombination (Seager, Sasselov, & Scott 2000) and from partial reionization prior to z_r by the first stars (Venkatesan, Tumlinson, & Shull 2003) and early X-ray sources (Venkatesan, Giroux, & Shull 2001; Ricotti & Ostriker 2004). These additional ionization sources could contribute extra electron scattering in the amount $\Delta\tau_e \approx 0.02$. We now invert the above relation to estimate the reionization redshift,

$$(1+z_r) \approx (16.2) \left(\frac{\tau_e}{0.15}\right)^{2/3}. \quad (4)$$

Here, we scaled to $\tau_e = 0.15$, equal to the WMAP-measured value of optical depth, $\tau_e = 0.17 \pm 0.04$, reduced by $\Delta\tau_e = 0.02$ arising from additional electron

scattering prior to z_r . A re-analysis of WMAP data (Tegmark et al. 2004), including prior knowledge of the SDSS galaxy power-spectrum, found slightly lower optical depth, $\tau_e = 0.124_{-0.057}^{+0.083}$ and reionization at $z_r = 14.4_{-4.7}^{+5.2}$. The large (1σ) likelihood range allows an optical depth near the value, $\tau_e \approx 0.05$, expected from from eq. (4), assuming a reionization epoch $z_r \approx 6 - 7$ consistent with H I Ly α opacity. The agreement would be particularly good if one allows for sources of partial ionization at $z > z_r$.

3. FUSE Observations of He II Absorbers

Over the last decade, IGM studies have been enhanced by high-resolution optical and UV spectra of quasar absorption lines. Studies in H I and He II Ly α are particularly important for understanding the transition of the high-redshift IGM from a neutral to ionized medium. The He II absorption becomes detectable in the far ultraviolet at redshifts $z \geq 2.03$ with *FUSE* and at $z \geq 2.79$ with the *Hubble Space Telescope* (HST). Moderate-resolution *FUSE* spectra of He II absorption (Kriss et al. 2001; Shull et al. 2004; Zheng et al. 2004) confirm the general theoretical picture (Cen et al. 1994; Davé et al. 2001) of the IGM as a fluctuating distribution of baryons, organized by the gravitational forces of dark matter and photoionized by high-redshift quasars and starburst galaxies (Haardt & Madau 1996; Fardal, Giroux, & Shull 1998, hereafter FGS).

The He II reionization epoch appears to occur at $z \approx 2.8 \pm 0.2$ (Kriss et al. 2001; Smette et al. 2002; Shull et al. 2004), based on several sightlines studied with HST and *FUSE*. This effect is demonstrated in Figure 1, which shows the patchy regions of broad-band (He II Ly α) opacity between $z = 2.7 - 2.9$ toward the QSO HE 2347-4342. Helium reionization is delayed by 1.4 Gyr ($\Delta z \approx 3$) from hydrogen reionization, probably because He II is more difficult to ionize, requiring a harder (4 ryd continuum), probably from AGN. It is also possible that partial He II reionization could occur at $z > 6$, from a population of ultra-hot, zero-metallicity massive stars (Tumlinson & Shull 2000; Venkatesan, Tumlinson, & Shull 2003).

FUSE observations of He II can be combined with the corresponding H I Ly α lines at optical wavelengths, to yield the ratio, $\eta = N(\text{He II})/N(\text{H I})$. As we explain, measurements of η probe the shape of the high-redshift metagalactic radiation field, presumably from quasars and massive stars. Figure 2 shows a portion of the combined observations of He II and H I absorption for the Ly α forest at $z \approx 2.3 - 2.6$. The He II absorption is generally much stronger than H I by a factor $\eta = N(\text{He II})/N(\text{H I})$, predicted theoretically (FGS) to be 50–100 for photoionization by quasar backgrounds. For optically thin lines, we can write $\eta \approx 4\tau_{\text{HeII}}/\tau_{\text{HI}}$. The greater strength of He II arises because it is harder to photoionize than H I, owing to lower fluxes and cross sections at its ionizing threshold ($h\nu_T = 54.4$ eV) and because He III recombines 5 times faster than H II. Variations in η can be used to diagnose the sources and fluctuations of the metagalactic ionizing spectrum in the continua of H I (1 ryd) and He II (4 ryd). He II absorption is also a good diagnostic of absorption from low-density regions (“voids”) in the IGM. Because $\tau_{\text{HeII}} = (\eta/4)\tau_{\text{HI}}$ ($\eta \gg 1$), He II can be tracked into much lower density regions than H I. He II absorption can also be used to

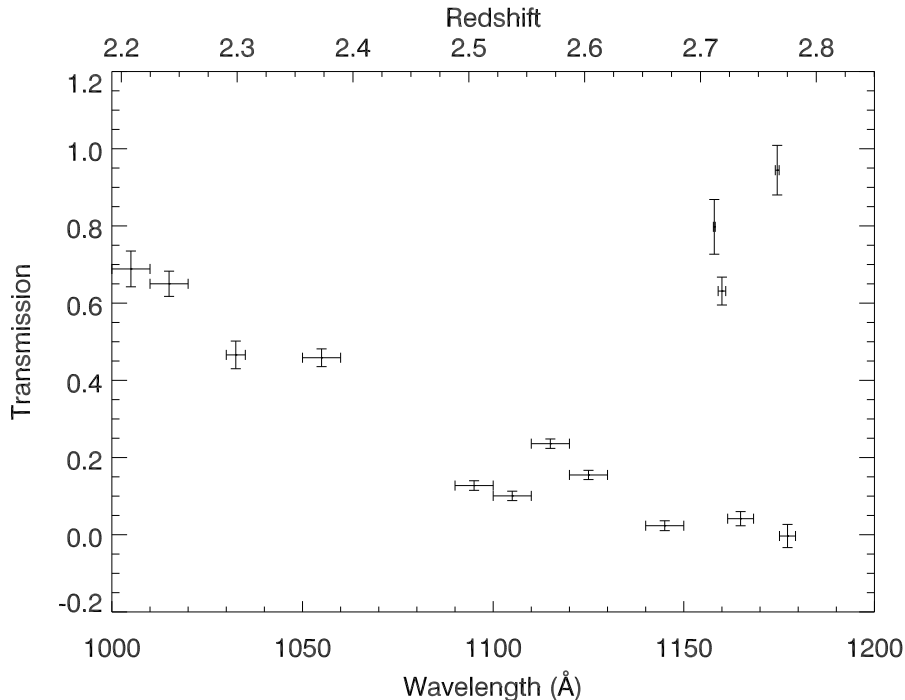


Figure 1. The epoch of gradual He II reionization at $z_{\text{HeII}} \approx 2.8 \pm 0.2$ toward HE 2347-4342 (Shull et al. 2004) is illustrated by the continuum flux transmission through He II absorption in several well-defined redshift windows. Note the three regions of high transmission between $z = 2.7 - 2.8$, flanked by low transmission regions. The transmission slowly recovers at $z < 2.6$.

probe collisionally ionized gas at $T \approx 10^5$ K, produced by shock-heating during structure formation (Cen & Ostriker 1999; Davé et al. 2001).

Following the initial *FUSE* discovery and analysis paper (Kriss et al. 2001), Shull et al. (2004) and Zheng et al. (2004) performed in-depth analyses of the He II and H I absorption toward HE 2347-4342, an AGN at redshift $z_{\text{em}} = 2.89$. We probed the IGM at redshifts $z = 2.3-2.9$, using spectra from *FUSE* and the *Ultraviolet-Visual Echelle Spectrograph* (UVES) on the VLT telescope. We focussed on two major topics: (1) small-scale variability ($\Delta z \approx 10^{-3}$) in the ratio $\eta = N(\text{He II})/N(\text{H I})$; and (2) an observed correlation of high- η absorbers (soft radiation fields) with voids in the (H I) Ly α distribution. These η variations (Figure 3) probably reflect fluctuations in the ionizing sources on scales of 1 Mpc, modified by radiative transfer through a filamentary IGM whose opacity controls the penetration of 1-5 ryd radiation over 30-40 Mpc distances. In photoionization equilibrium, the He II/H I ratio can be expressed:

$$\eta = \frac{n_{\text{HeIII}} \alpha_{\text{HeII}}^{(A)} \Gamma_{\text{HI}}}{n_{\text{HII}} \alpha_{\text{HI}}^{(A)} \Gamma_{\text{HeII}}} \approx (1.70) \frac{J_{\text{HI}} (3 + \alpha_4)}{J_{\text{HeII}} (3 + \alpha_1)} T_{4.3}^{0.055}. \quad (5)$$

Here, $\alpha_{\text{HI}}^{(A)}$, $\alpha_{\text{HeII}}^{(A)}$, Γ_{HI} , and Γ_{HeII} are the case-A recombination rate coefficients and photoionization rates for H I and He II, and J_{HI} and J_{HeII} are the specific

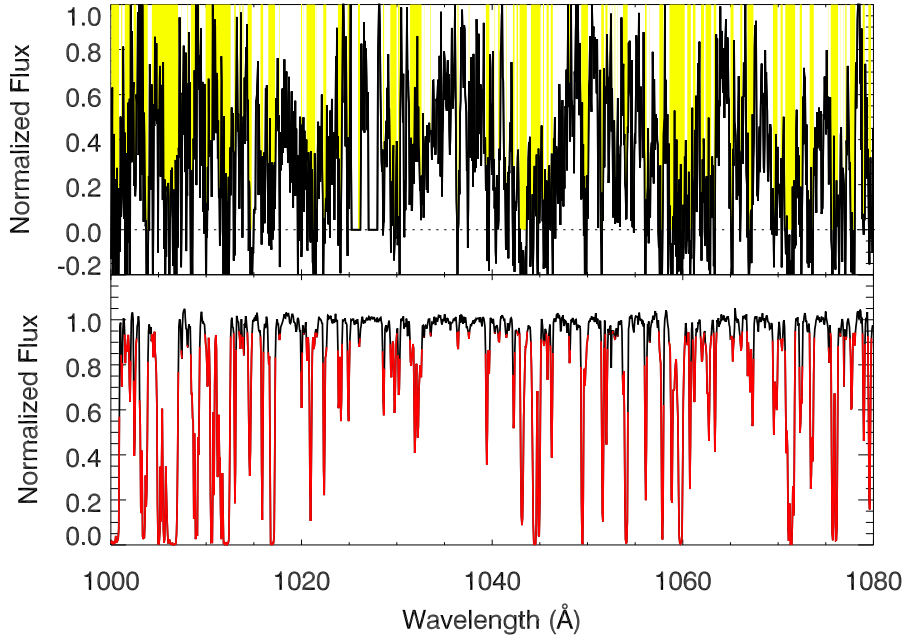


Figure 2. Overlay of the Ly α absorption of He II (top panel – *FUSE*) and of H I (bottom panel – VLT/*UVES*) toward HE 2347-4342. In the VLT data, “filament” points are defined as those with $\tau_{\text{HI}} > 0.05$. Wavelengths of H I Ly α were divided by 4 for alignment. Note the strong He II absorption (top).

intensities of the radiation field at the H I (912 Å) and He II (228 Å) edges. The parameters α_1 and α_4 are the local spectral indices of the ionizing background at 1 and 4 ryd, respectively, which provide minor corrections to the photoionization rates. We adopt case-A hydrogenic recombination rates to H I and He II, appropriate for the Ly α forest absorbers with very low neutral fractions. Over the temperature range $16,000 \text{ K} < T < 32,000 \text{ K}$, we approximate the case-A recombination rates coefficients as $\alpha_{\text{HeII}} = (1.36 \times 10^{-12} \text{ cm}^3 \text{ s}^{-1}) T_{4.3}^{-0.700}$ and $\alpha_{\text{HI}} = (2.51 \times 10^{-13} \text{ cm}^3 \text{ s}^{-1}) T_{4.3}^{-0.755}$, where $T_{4.3} \equiv (T/10^{4.3} \text{ K})$. We assume that $n_{\text{He}}/n_{\text{H}} = 0.08$ ($Y = 0.244$) and that H and He are fully ionized ($n_e = 1.16n_H$) after reionization ($z < 3$).

Owing to photon statistics and backgrounds, we can measure optical depths over the ranges $0.1 < \tau_{\text{HeII}} < 2.3$ and $0.02 < \tau_{\text{HI}} < 3.9$, and we can reliably determine values of $\eta \approx 4\tau_{\text{HeII}}/\tau_{\text{HI}}$ over the range 0.1 to 460. Values $\eta = 20 - 200$ are consistent with models of photoionization by quasars with observed spectral indices ranging from $\alpha_s = 0 - 3$ (Figure 4). Values $\eta > 200$ may require additional contributions from starburst galaxies, heavily filtered quasar radiation, or density variations. Regions with $\eta < 30$ may indicate the presence of local hard sources. We find that η is higher in “void” regions, where H I is weak or undetected and $\sim 80\%$ of the path length has $\eta > 100$. These voids may be ionized by local soft sources (dwarf starbursts) or by QSO radiation

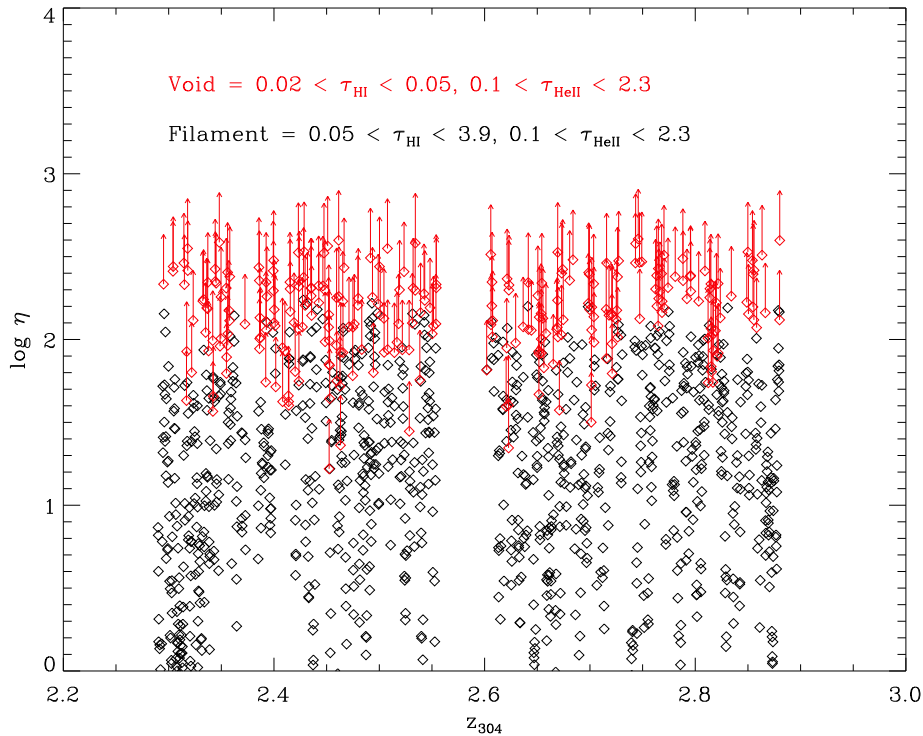


Figure 3. Observed wide variations in the ratio $\eta = N(\text{He II})/N(\text{H I})$ in the IGM toward HE 2347-4342 (Shull et al. 2004). These variations imply substantial fine-grained fluctuations in the ionizing radiation field at 1 ryd (H I) and 4 ryd (He II) on scales of $\Delta z = 0.001$ or 1 Mpc.

softened by escape from the AGN cores or transfer through the “cosmic web”. The apparent differences in ionizing spectra may help to explain the 1.4 Gyr lag between the reionization epochs of H I ($z_{\text{HI}} \sim 6.1 \pm 0.3$; Gnedin 2004) and He II ($z_{\text{HeII}} \sim 2.8 \pm 0.2$; Kriss et al. 2001; Shull et al. 2004).

Many of the variations in the ionizing radiation field appear to come from intrinsic differences in QSO spectra (Fig. 4), found by direct measurements of the redshifted EUV continua using HST (Telfer et al. 2002) and *FUSE* (Scott et al. 2004). Figure 5 shows some of the actual AGN spectra on which these conclusions are based. It is apparent that even low-redshift QSOs and Seyferts have wide differences in their EUV continuum slopes, which may be luminosity dependent (Scott et al. 2004). In addition to intrinsic source variations, the metagalactic radiation field is heavily filtered and reprocessed by intervening IGM (see FGS). Because the He II opacity is so strong ($\eta \gg 1$), fluctuations at 4 ryd are probably larger than those at 1 ryd. Unfortunately, we must conclude that the sources, spectra, and fine-grained spatial variations in the metagalactic ionizing radiation field are still not well understood.

Future studies of He II should proceed along several fronts. First and foremost, we need to find additional high-redshift AGN targets for which we can

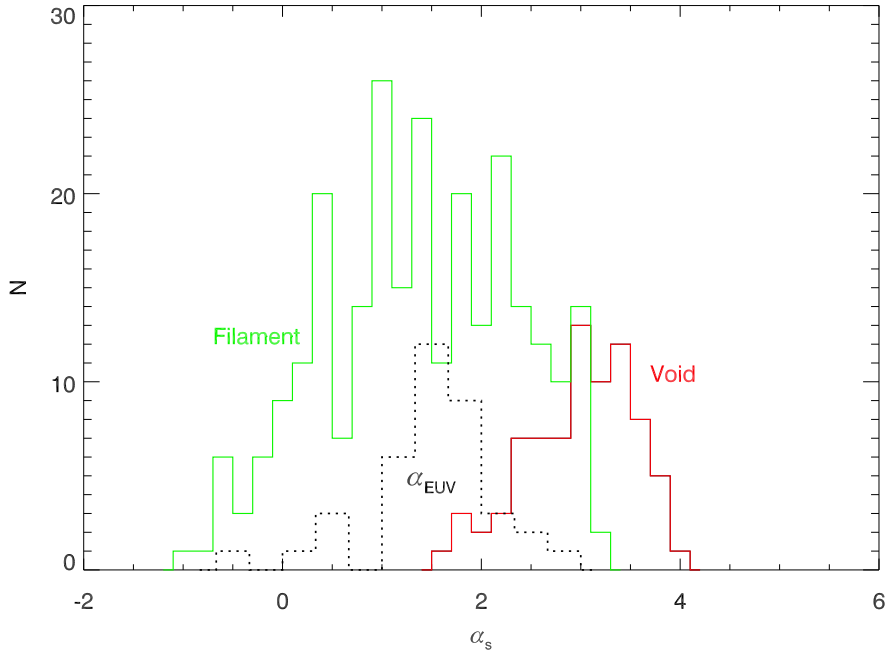


Figure 4. Observed distribution of the observed QSO ionizing spectral indices, α_{EUV} , for radio-quiet AGN observed by HST (Telfer et al. 2002). Other curves show the spectral indices α_s , with $J_\nu \propto \nu^{-\alpha_s}$, that are required to reproduce the observed values of He II/H I ratios, using eq. [5]. Note the systematically softer radiation fields (high η , large α_s) in the voids ($\tau_{\text{HI}} < 0.05$) compared to filaments ($\tau_{\text{HI}} > 0.05$). The breadth of these distributions and the clear offset between voids and filaments suggest that additional spectral softening may be present.

repeat the He II/H I measurements and η analysis. Quasar H1700+6416 at $z_{\text{em}} = 2.74$ is one such *FUSE* target, but more are needed to identify the cosmic variance in $z_r(\text{He II})$. Additional theoretical work is needed, using cosmological simulations that include radiative transfer of the 1 ryd and 4 ryd radiation intensities and their spatial fluctuations. Radiation in the 3-4 ryd band may be especially important for the photoionization corrections to C III, C IV, Si III, and Si IV on which IGM metallicities are based. Finally, it would be helpful to characterize the mean intrinsic EUV spectra of AGN, at $z \leq 0.5$, which are still highly uncertain (Figure 5) despite heroic efforts with both HST and *FUSE*. There is currently only a small wavelength window at which the rest-frame EUV is observable, and it does not extend to $\lambda \leq 228 \text{ \AA}$, the 4 ryd continuum that controls He II ionization.

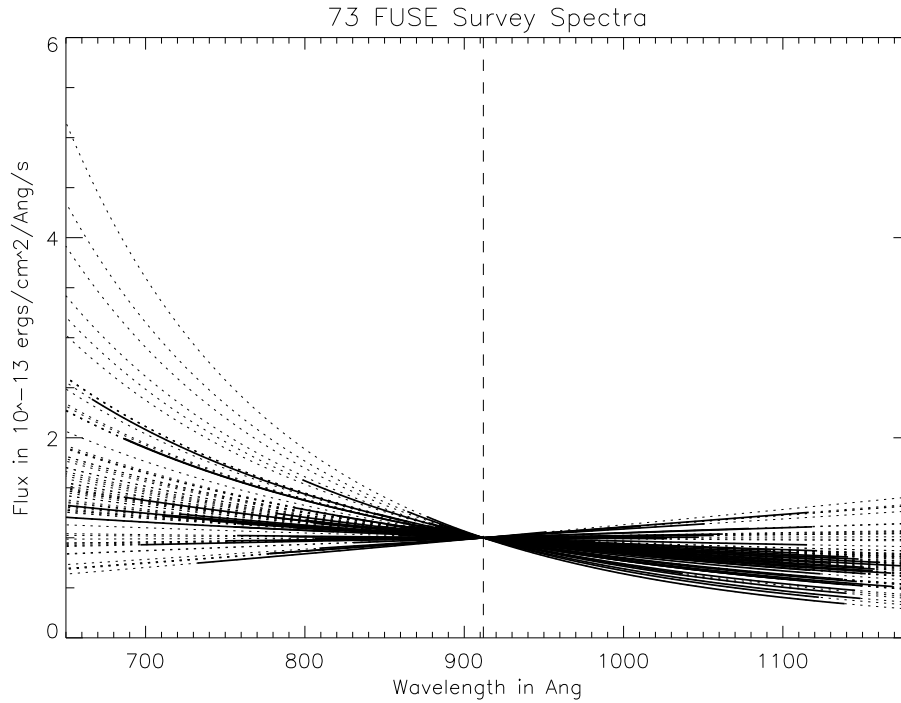


Figure 5. Normalized distribution of fits to the rest-frame UV and EUV continuum spectra of 73 AGN (Clausen & Shull 2004), taken from *FUSE* data analyzed and fitted by Scott et al. (2004). We have shifted these data to the rest-frame, K-corrected the UV fluxes, and normalized them to unity at 1 ryd (912 Å). The solid lines show actual data, and dotted lines are extrapolations. Note the wide variations in spectral indices at $\lambda = 650 - 900$ Å.

References

- Becker, R., et al. 2001, *AJ*, 122, 2850
 Bennett, C. L., et al. 2003, *ApJS*, 148, 1
 Cen, R., Miralda-Escudé J., Ostriker, J. P., & Rauch, M. 1994, *ApJ*, 437, L9
 Cen, R., & Ostriker, J. P. 1999, *ApJ*, 519, L109
 Clausen, D., & Shull, J. M. 2004, *ApJ*, in preparation
 Davé, R., et al. 2001, *ApJ*, 511, 521
 Fan, X., et al. 2002, *AJ*, 123, 1247
 Fardal, M. A., Giroux, M. L., & Shull, J. M. 1998, *AJ*, 115, 2206 (FGS)
 Gnedin, N. Y. 2000, *ApJ*, 535, 530
 Gnedin, N. Y. 2004, *ApJ*, 610, 9
 Haardt, F., & Madau, P. 1996, *ApJ*, 461, 20
 Kogut, A., et al. 2003, *ApJS*, 148, 161
 Kriss, G. A., et al. 2001, *Science*, 293, 1112
 Ricotti, M., Gnedin, N. Y., & Shull, J. M. 2002, *ApJ*, 575, 49 (RGS)
 Ricotti, M., & Ostriker, J. P. 2004, *MNRAS*, 353, 547
 Scott, J. E., et al. 2004, *ApJ*, 615, in press (Nov. 1 issue)
 Seager, S., Sasselov, D. D., & Scott, D. 2000, *ApJS*, 128, 407
 Shull, J. M., et al. 2004, *ApJ*, 600, 570
 Smette, A., et al. 2002, *ApJ*, 564, 542

- Songaila, A. 1998, ApJ, 561, L153
Spergel, D. N., et al. 2003, ApJS, 148, 175
Steidel, C. C., et al. 2002, ApJ, 570, 526
Tegmark, M. et al. 2004, Phys. Rev. D, 69, 103501
Telfer, R., Zheng, W., Kriss, G. A., & Davidson, A. F. 2002, ApJ, 565, 773
Tumlinson, J., & Shull, J. M. 2000, ApJ, 528, L65
Venkatesan, A., Giroux, M. L., & Shull, J. M. 2001, ApJ, 563, 1
Venkatesan, A., Tumlinson, J., & Shull, J. M. 2003, ApJ, 584, 621
Zheng, W., et al. 2004, ApJ, 605, 631